# Structural Design of Connecting Rod Thumb Rehabilitation Exoskeleton

Lingjia Li

West China School of Medicine, Sichuan University, Chengdu, China

2022141410378@scu.edu.cn

**Abstract.** This paper addresses the rehabilitation needs of thumb motor disorders in stroke patients by proposing a lightweight thumb rehabilitation exoskeleton based on rigid linkages. The study first analyzed the anatomical characteristics and motion mechanisms of the thumb, clarified the range of motion and torque characteristics of each thumb joint, and established a joint angle trajectory model. Based on this, a four-degree-of-freedom (DOF) linkage-based thumb exoskeleton was designed, capable of performing key movements such as opposition, flexion and extension, and pronation. The structure utilizes Bowden cables for remote actuation to reduce hand load, and kinematic and static models were established through geometric mapping and Jacobian matrix analysis. Simulation results demonstrate that the exoskeleton's output torque covers the range of human physiological requirements, and its motion trajectory is highly consistent with natural thumb movement. This design enables precise and repeatable thumb rehabilitation training for stroke and neurological injury patients, improving rehabilitation efficiency and safety. The study also noted that rigid linkage structures still have limitations in terms of human-machine compatibility and compliance. Future work will aim to optimize the exoskeleton's ergonomic performance and biomimetic features by combining flexible materials with intelligent control algorithms.

**Keywords:** Thumb exoskeleton; rehabilitation engineering; thumb motor function.

## 1. Introduction

Stroke is one of the leading causes of long-term disability worldwide, bringing a huge economic burden [1]. Studies have shown that more than 80% of patients will experience contralateral upper limb motor disorders during the acute phase, with impairment of fine motor skills in the hands being particularly prominent [2]. The thumb plays an important role in achieving hand functions. Studies have shown that the thumb is involved in more than 50% of hand movements [3]. Stroke patients often experience flexion spasm or extension weakness in their thumbs, making it difficult to perform fine manipulations [4]. This can severely impact patients' daily living abilities and independence. So restoring thumb function is of great significance.

The effectiveness of traditional treatments depends on the therapist's experience, and there are problems such as limited training intensity, heavy labor burden, and insufficient patient compliance [5].

Recently, hand exoskeletons have gradually developed, providing ideas for achieving controllable, repetitive, and quantitative training for fingers. The research on hand exoskeletons is divided into rigidity and flexibility. Although flexible exoskeletons have good wearability and safety, their output force and accuracy are limited, and their durability is insufficient [6]. In contrast, the rigid link structure has more advantages in motion control and predictability [6]. In addition, the modular design of the link mechanism makes it easier to adjust parameters according to individual differences, which widens the applicability.

However, the Link Thumb Exoskeleton still faces many challenges. For example, individual differences and slippage within the carpometacarpal joint cause deviations in the exoskeleton-physiological axis, which affects the alignment of the human-machine axis. The space occupied by the connecting rod and the integration of components can easily affect ease of use and wearing comfort.

This paper aims to propose a thumb exoskeleton rehabilitation robot based on a connecting rod structure to simulate the physiological movement of the thumb, which can realize thumb-to-palm movement, and each joint is independently driven.

## 2. Hand Exoskeleton Design

### 2.1. Analysis of Thumb Movement

#### 2.1.1 Anatomy of the thumb joint

Fig. 1 shows the bone and joint features of the thumb. The thumb bones originate from the trapezium (T) at the wrist, and connect to the metacarpus (M), proximal phalanges (Pp), and distal phalanges (Pd). The key joints are the carpometacarpal joint (CMC), the metacarpophalangeal joint (MCP), and the interphalangeal joint (IP). The CMC enables flexion/extension, adduction/abduction, and palmar alignment/reduction. The MCP can perform flexion, extension, and a small amount of lateral movement. The IP is responsible for flexion/extension.

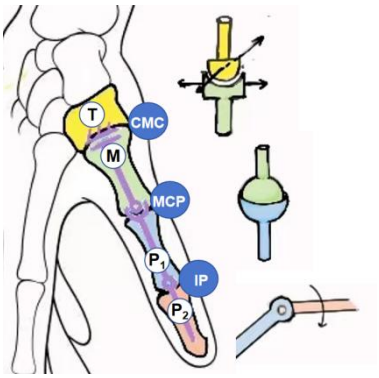


**Fig. 1** Thumb Skeletal Anatomy (Picture credit: Original)

#### 2.1.2 Analysis of thumb palm movement

Thumb opposition is the core of thumb function. Its essence is that the thumb tip moves toward the ulnar and palmar sides, thereby contacting the tips of other fingers to achieve pinching [7]. The process begins with the CMC adducting the thumb to the palm; the CMC, MCP, and IP flex to complete the closure; through the asymmetry of the CMC joint surface and the ligament laxity, the thumb produces passive rotation to achieve palmar movement [8].

Fig. 2 shows the core muscles involved in the movement of the palms. The opponens pollicis muscle directly carries out the movement. When it contracts, the first metacarpal internally rotates and moves forward [9]. The adductor pollicis helps the thumb maintain a stable contact position during the later stages of the palm-to-palm movement [10].

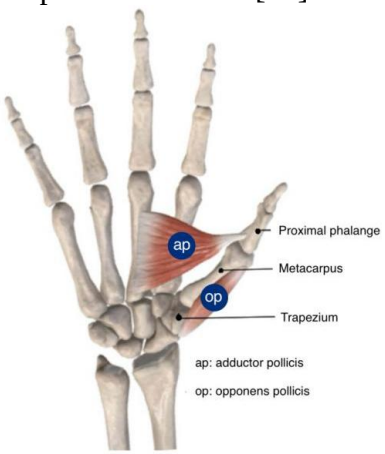


**Fig. 2** Opponents pollicis and adductor pollicis muscles (Picture credit: Original)

### 2.1.3 Thumb kinematics

The length of bones of thumb bones is mainly determined based on the skeletal measurements in healthy adults [11]. In terms of joint motion angles, the IP flexion is about 80–90°, the MCP flexion is about 43–70°, the CMC flexion and extension are about 53°, and abduction/adduction is about 42° [12]. During the palm-opposing movement, the M produces an axial rotation of about 56° when it is reduced to the position of opposing the little finger. Mechanical studies show that the joint torque is approximately within the range of 0.2 to 0.7 N·m, which is sufficient to achieve a stable fingertip force [13] [14] [15]. In summary, the CMC bears the primary load, while the MCP and IP primarily participate in flexion and extension. The kinematic indices are summarized in Table 1.

**Table 1.** Length of each part of the thumb and physiological indicators of the joints

| | | Length(mm) | |
|---|---|---|---|
| PP | | 31.57±3.13 | |
| Pd | | 21.67±1.60 | |
| M | | 5.67±0.61 | |
| Joint | Motion | ROM | Torque |
| IP | Flexion | 80-90° | 0.3-0.7 |
| | Extension | 0-45° | |
| MCP | Flexion | 43-70° | 0.17–0.6 |
| | Extension | 0-15° | |
| CMC | Abduction/Adduction | ~42° | 0.6 |
| Metacarpal | Axial Rotation (opposition) | ~56° | 0.6 |

In thumb kinematic modeling, the variation of joint angles over time can be described by quintic polynomial trajectory planning, which can ensure the continuity and smoothness of the function. The joint Angle functions of the flexion and extension movements of each joint of the thumb are as follows.

$$\theta(t) = a_0 + a_1 t + a_2 t^2 + a_3 t^3 + a_4 t^4 + a_5 t^5 \quad (1)$$

$a_0$~$a_5$is the trajectory planning coefficient.

Angular velocity and angular acceleration are obtained by differentiation:

$$\dot{\theta}(t) = a_1 + 2a_2 t + 3a_3 t^2 + 4a_4 t^3 + 5a_5 t^4 \quad (2)$$

$$\ddot{\theta}(t) = 2a_2 + 6a_3 t + 12a_4 t^2 + 20a_5 t^3 \quad (3)$$

## 2.2. Thumb Exoskeleton Design

### 2.2.1 Design Requirements

As exoskeleton rehabilitation robots need to be in direct contact with the human body, their structure should have good adaptability to the size of the hand, operational safety, wearing comfort and as economical as possible.

Based on the analysis of the above chapters, the mechanism can be simplified to three nodes and four degrees of freedom, where IP is parallel to the rotation axis of MCP and orthogonal to the rotation axis of CMC.

### 2.2.2 Structural design

From the above analysis, it can be known that the main movement forms of thumb MCP and IP are different from those of CMC, so they need to be considered separately. Fig. 3 shows the three-dimensional model of this mechanism(a) and the wear effect. The design is described below.

(1) IP/MCP

The IP is relatively stable, and the muscles around the two phalanges are thinner than those in the rest of the thumb. Considering the size of the thumb, the connecting rod is placed laterally to facilitate alignment and prevent interference.

The MCP is relatively flexible, the metacarpal bones are rich in muscles, and it uses a dorsal exoskeleton. The main body changes one of the rotating pairs of the hinged four-bar mechanism into a moving pair to compensate for the directional component; a rocker arm is added to the rotating pair close to the metacarpal bone to supplement the lateral offset during movement and ensure that the mechanism's force is perpendicular to the finger.

(2) CMC

Due to the unique characteristics of the CMC, the center of rotation of the pendulum arm is placed directly on the joint. Connected to the thumb rest via a cylindrical pair, this allows for axial rotation of the metacarpal bone. A single link connects the CMC base to the palm rest, driving metacarpal rotation and completing one step of the palmar movement.

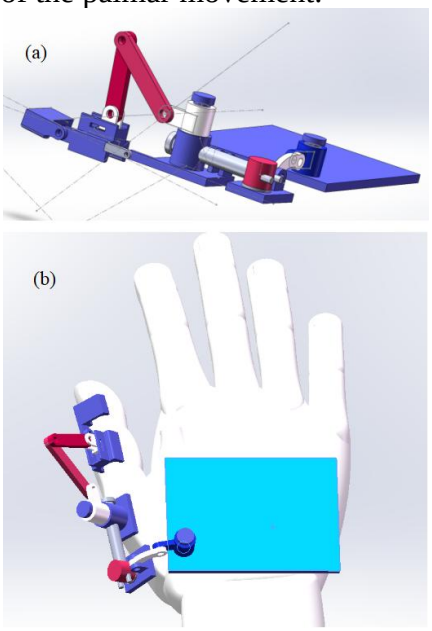


**Fig. 3** Three-dimensional model of the overall structure (Picture credit: Original)

### 2.2.3 Selection of transmission mode

The Bowden cable is a flexible transmission mechanism consisting of an inner wire and an outer sheath that transmits mechanical force through cable tension. When the driver retracts the cable, the inner wire slides within the sheath to produce joint flexion, and extension is achieved via an elastic element. In this study, a Bowden cable is employed for remote actuation to decouple the heavy driving unit from the wearable structure, thereby reducing human–device interference and enhancing comfort. Moreover, its flexibility allows multidirectional motion transmission, meeting the thumb's motion requirements across multiple planes.

## 2.3. Kinematic and Mechanical Analysis

The thumb exoskeleton can achieve CMC adduction/abduction, MCP extension/flexion, IP extension/flexion, and M pronation. A simplified diagram of the overall exoskeleton and MCP joint is shown in Fig. 4.

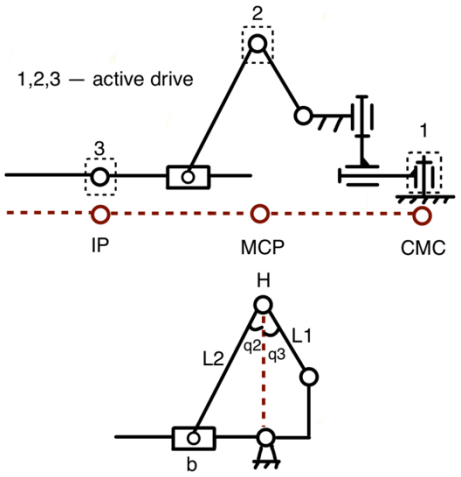


**Fig. 4** Simple diagram of the mechanism's movement (Picture credit: Original)

### 2.3.1 Kinematics

(1) Overview of the kinematics of the overall structure

The mechanism is modeled using the Denavit-Hartenberg method with the three main joints of the thumb as generalized coordinates; the DH parameter table is shown in Table 2. The main symbols are defined as follows: Li indicates the length of the connecting rod in the i-th section, αi is the connecting rod torsion angle, di is the connecting rod offset, $\theta_i$ is the connecting rod angle. Through the homogeneous transformation matrix $T_i^{i-1}$, which can realize the spatial mapping from the i-1th coordinate system to the i-th coordinate system.

**Table 2.** DH parameters of the main joints of the thumb

| Joint | Li{mm} | $\alpha$i{rad} | di(mm) | $\theta_i$ |
|---|---|---|---|---|
| CMC | 0 | $-\frac{\pi}{2}$ | 0 | $\theta_1$ |
| MCP | L1 | 0 | 0 | $\theta_2$ |
| IP | L2 | 0 | 0 | $\theta_3$ |
| Tip | L3 | 0 | 0 | 0 |

$$T = \prod_{i=1}^{3} T_i \tag{4}$$

$$T_i = \begin{bmatrix} \cos\theta_i & -\sin\theta_i \cos\alpha_i & \sin\theta_i \sin\alpha_i & \alpha_i \cos\theta_i \\ \sin\theta_i & \cos\theta_i \cos\alpha_i & -\cos\theta_i \sin\alpha_i & \alpha_i \sin\theta_i \\ 0 & \sin\alpha_i & \cos\alpha_i & d_i \\ 0 & 0 & 0 & 1 \end{bmatrix} \tag{5}$$

The thumb tip position vector p can be expressed as,

$$p = \begin{bmatrix} x \\ y \\ z \end{bmatrix} = f(\theta_1, \theta_2, \theta_3) \tag{6}$$

Its geometric form is,

$$x = L_1 \cos\theta_1 + L_2 \cos(\theta_1 + \theta_2) + L_3 \cos(\theta_1 + \theta_2 + \theta_3) \tag{7}$$

$$y = L_1 \sin\theta_1 + L_2 \sin(\theta_1 + \theta_2) + L_3 \sin(\theta_1 + \theta_2 + \theta_3) \tag{8}$$

$$z = 0 \text{(Decomposition into planar motion)} \tag{9}$$

Slider b displacement mapping s(q)

1) Geometric expression

Let q1 be the CMC adduction/abduction angle (about the base Z axis, rad). q4 is the metacarpal pronation angle (about the metacarpal longitudinal axis, rad). q2 and q3 are the angles of link 1 and link 2 relative to the baseline at the MCP flexion joint at the connection point H.

The position of point H is determined using a forward kinematic geometric formula, abbreviated as

$$p_H(q_1, q_4) = R_{base}(q_1, q_4)\begin{bmatrix} d_{CH} \\ 0 \\ 0 \end{bmatrix} + \begin{bmatrix} 0 \\ 0 \\ h_{rise} \end{bmatrix} \tag{10}$$

Where

$$R_{base}(q_1, q_4) = R_Z(q_1)R_{axis}(u_m, q_4) \tag{11}$$

um is the unit vector in the direction of the metacarpal bone. The global coordinate of the slider is

$$p_b(q) = p_H(q_1, q_4) + R_{base}(q_1, q_4)r_{Hb}(q_2, q_3) \tag{12}$$

Where

$$r_{Hb}(q_2, q_3) = \begin{bmatrix} x_H(q_2, q_3) \\ y_H(q_2, q_3) \\ z_H \end{bmatrix} \tag{13}$$

2) Slider displacement

$$s(q) = u_s{}^{\top}(p_b(q) - p_{slot0}) \tag{14}$$

us is the slider lead, pslot0 is the slider zero point.

3)Slider-Joint Jacobian

$$J_s(q) = \nabla_q s = \left[\partial_s/\partial_{q_1} \;\; \partial_s/\partial_{q_4} \;\; \partial_s/\partial_{q_2} \;\; \partial_s/\partial_{q_3}\right] \tag{15}$$

4)MCP angular velocity jacobian

Using the arc approximation, the composite derivative of s(q) can be obtained to obtain the MCP angular velocity Jacobian:

$$J_\emptyset(q) = \frac{1}{d_m \sin\phi(q)} J_s(q) \tag{16}$$

Mapping of connecting rod angle to MCP

Directly obtain partial derivatives from the composite function$\phi(q) = \phi\big(s(q)\big)$

$$\frac{\partial_\varphi}{\partial q_i} = \frac{1}{d_m \sin\phi} u_s^{\top} R_{base}(q_1, q_4)\begin{bmatrix} -L_{(i-1)} \sin q_i \\ L_{(i-1)} \cos q_i \\ 0 \end{bmatrix} \tag{17}$$

### 2.3.2 Mechanical analysis

Since the required running speed during rehabilitation training is relatively slow, only static analysis is performed here.

MCP-two-link-slider mechanism has a torque balance formula,

$$T_{MCP} = F_{in} \cdot r \cdot \sin\varphi \tag{18}$$

Where$F_{in}$ represents the input force, r is the lever arm of the single link-slider hinge, and $\varphi$ is the angle between the link and the slide. According to the actual mechanical characteristics of the Bowden cable transmission, the joint output torque is determined by the input tension, winding radius and friction attenuation, which can be expressed as

$$T_{out} = F_{in} r_0 \cos(\theta) e^{-\mu k_\alpha \theta} \tag{19}$$

## 3. Simulation analysis

Fig. 5 shows the kinematic response of the thumb exoskeleton from 0 to 2 s and its comparison with the range of motion (ROM) of the human thumb. Fig. 5(a) shows the relationship between the angle, angular velocity and angular acceleration of the CMC, MCP and IP over time. The results showed that the angular displacement curves of the three joints rose smoothly, with maximum angles of approximately 90°, 40°, and 60°, respectively. The angular velocity showed a unimodal distribution, with peak values of approximately 85°/s, 70°/s, and 55°/s, reflecting the acceleration-deceleration characteristics of the movement. The angular acceleration curve showed positive and negative pulses during the starting and braking phases, corresponding to the dynamic transitions of the joints. In the Fig. 5(b), the exoskeleton simulation trajectory (blue) and the human reference trajectory (red) almost completely overlap, with a coverage rate of 100%, indicating that the kinematic design of the mechanism can effectively reproduce the physiological motion range and coordination characteristics of a natural thumb.

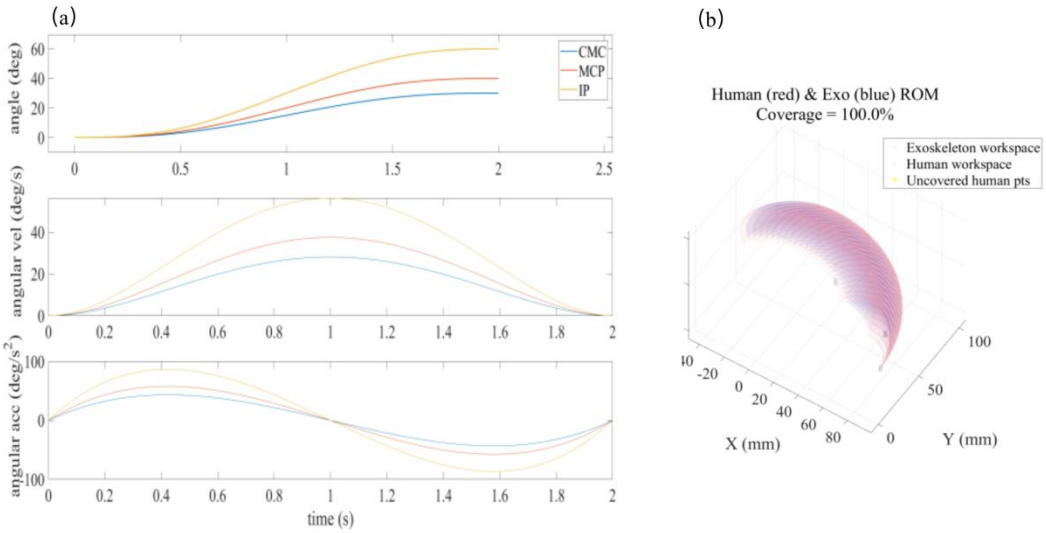


**Fig. 5** Changes in angles, angular velocities, and angular accelerations of the thumb exoskeleton joints and their comparison with the human range of motion (ROM) (Picture credit: Original).

Fig. 6 shows the variation of the output torque of each thumb joint of the exoskeleton with the flexion angle. The horizontal axis represents joint flexion angle (°), and the vertical axis represents torque (N·m). The blue, orange, and yellow curves in Fig. 6 correspond to the torque outputs of the CMC, MCP, and IP joints. The red dashed line indicates the upper limit of the physiological torque for each joint. The horizontal axis represents joint flexion angle (°), and the vertical axis represents torque (N·m). The blue, orange, and yellow curves in Fig. 6 correspond to the torque outputs of the three joints. The red dashed line indicates the upper limit of the physiological torque for each joint. Comparing the exoskeleton's output torque to the upper limit of human physiological torque shows that it can fully meet physiological needs within a small to medium angle range. This result demonstrates that, under the conditions of reasonable control of input tension and friction coefficient, this design can provide sufficient joint assist torque.

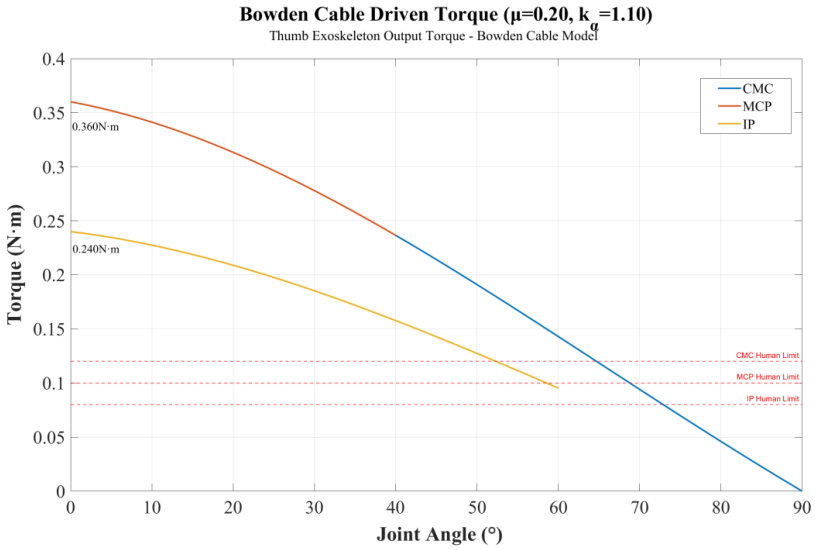


**Fig. 6** Simulated output torque–angle curves of the thumb exoskeleton joints (Picture credit: Original)

## 4. Conclusion

This study optimized the design of a traditional linkage mechanism and proposed a lightweight linkage exoskeleton that can achieve thumb-to-palm movement and adapt to dynamic changes in the joint's center of rotation. This approach aims to better simulate the physiological movement mechanism of the thumb. Based on the anatomical structure and kinematic characteristics of the thumb and the functional requirements of thumb-to-palm movement, the physiological model was rationally simplified to provide a theoretical basis for mechanism design. Simulation analysis confirmed that the mechanism's trajectory covered the main angle ranges required for typical thumb-to-palm movement in the literature. The torque met the required rehabilitation torque.

This exoskeleton can be used to assist patients with hand dysfunction with thumb rehabilitation training, improving training efficiency and consistency while also reducing the human resource burden during rehabilitation. Furthermore, its modular design allows it to be integrated as a standalone thumb unit with a four-finger exoskeleton, ensuring system compatibility and cost-effectiveness.

However, the rigid link structure used in this study still has certain limitations in terms of motion flexibility, comfort and human-machine adaptability, and the single-point drive mode of the mechanism cannot fully simulate the muscle coordination mechanism under physiological conditions. To address these issues, subsequent research will focus on developing more precise control strategies and more efficient driving methods, and will focus on exploring new exoskeleton structures that combine rigidity and flexibility to further enhance their bionic performance and comfort in relation to human thumb movements.

## References

[1] Feigin V L, Brainin M, Norrving B, Martins S O, Pandian J, Lindsay P, Grupper F M, Rautalin I. World Stroke Organization: Global Stroke Fact Sheet 2025. International Journal of Stroke, 2025, 20: 132–144.

[2] Heo P, Gu G M, Lee S J, Rhee K, Kim J. Current hand exoskeleton technologies for rehabilitation and assistive engineering. International Journal of Precision Engineering and Manufacturing, 2012, 13: 807–824.

[3] Smaby N, Johanson M E, Baker B, Kenney D E, Murray W M, Hentz V R. Identification of key pinch forces required to complete functional tasks. Journal of Rehabilitation Research and Development, 2004, 41: 215–224.

[4] Lemmens R J, Timmermans A A, Janssen-Potten Y J, et al. Valid and reliable instruments for arm-hand assessment at ICF activity level in persons with hemiplegia. Stroke, 2014, 45: 3006–3010.

[5] Bardi E, Gandolla M, Braghin F, Resta F, Pedrocchi A L G, Ambrosini E. Upper limb soft robotic wearable devices: A systematic review. Journal of NeuroEngineering and Rehabilitation, 2022, 19: 87.

[6] Gherman B, Zima I, Vaida C, Tucan P, Pisla A, Birlescu I, Machado J, Pisla D. Robotic systems for hand rehabilitation—Past, present and future. Technologies, 2025, 13: 37.

[7] MacDermid J C, Roth J H, Richards R S. Distinguishing thumb opposition and reposition: Kinematic analysis of normal movements. Journal of Hand Therapy, 2014, 27: 102–110.

[8] Cooney W P, Chao E Y S. Biomechanical analysis of the thumb: A theoretical study. Journal of Bone and Joint Surgery. American Volume, 1977, 59: 27–36.

[9] Standring S. Gray's Anatomy: The Anatomical Basis of Clinical Practice (42nd ed.). Elsevier, 2021.

[10] Levangie P K, Norkin C C. Joint Structure and Function: A Comprehensive Analysis (6th ed.). F.A. Davis Company, 2020.

[11] Burianov O A, Kotiuk V. Morphometrics of the human thumb metacarpal bone. Folia Morphologica, 2010, 69: 231–235.

[12] Barakat M, Field J, Taylor J. The Range of Movement of the Thumb. HAND, 2013, 8.

[13] Arner J W, McClure P, Williams P N, Patel S H. Passive joint torque characteristics of the thumb carpometacarpal joint. Journal of Hand Surgery, 2015, 40: 1172–1179.

[14] Valero-Cuevas F J, Johanson M E, Towles J D. Towards a realistic biomechanical model of the thumb: The choice of kinematic description may be more critical than the solution method or the variability/uncertainty of musculoskeletal parameters. Journal of Biomechanics, 2003, 36: 1019–1030.

[15] Valero-Cuevas F J, Zajac F E, Burgar C G. Large index-fingertip forces are produced by subject-independent patterns of muscle excitation. Journal of Biomechanics, 1998, 31: 693–703.